Spatio-temporal variations of vegetation cover and its influence on surface air temperature change over the Yellow River Basin, China

Zhenyue Han [ID][a], Qiang Wu[a], Ruixun Lai[b], Shan-e-hyder Soomro[a], Dongru Hou[a] and Caihong Hu[a,*]

[a] School of Water Conservancy Science and Engineering, Zhengzhou University, Zhengzhou 450001, China
[b] Yellow River Institute of Hydraulic Research, Zhengzhou 450003, China
*Corresponding author. E-mail: hucaihong@zzu.edu.cn

[ID] ZH, 0000-0002-1839-6352

ABSTRACT

Northwest China has experienced dramatic changes in vegetation cover over the past few decades with the Yellow River Basin (YRB) being the most representative area. As the major climate-sensitive area in China, vegetation cover change is one reason for its impact on surface air temperature (SAT). This study uses the observation minus reanalysis (OMR) method to reveal the spatio-temporal variations of vegetation cover and its impact on SAT change over non-urban areas of the YRB from 1982 to 2015. The Global Inventory Modeling and Mapping Studies dataset, SAT derived from meteorological stations, and European Reanalysis (ERA)-interim reanalysis temperature data were used to analyze the relationship between normalized difference vegetation index (NDVI) and temperature variation caused by vegetation change. The NDVI trend ($Slope_{NDVI}$) of the entire YRB reached 1.11×10^{-2} decade^{-1}, which indicated the recovery of vegetation in general. The impact of variation in vegetation conditions on SAT change during 1982–2015 was estimated to be 0.037 °C decade^{-1}, which contributed 7.62% to the temperature change. The mean annual NDVI (M_{NDVI}) and $Slope_{NDVI}$ in the YRB were significantly negatively correlated ($P<0.001$) with OMR temperature variation. A negative correlation was exhibited in semi-arid and semi-humid regions, whereas a positive correlation was found in the arid region. The observed changes in vegetation and SAT in the YRB support the theory of the impact of vegetation variation on SAT in China.

Key words: non-urban area, observation minus reanalysis method, spatio-temporal variations of NDVI, surface air temperature change, Yellow River Basin

HIGHLIGHTS

- The relationship between vegetation and surface air temperature is different across the climate regions. The spatio-temporal changes of vegetation in non-urban areas of the Yellow River Basin were studied.
- The contribution rate of the surface air temperature changes caused by vegetation changes during 1982–2015 is 7.62%. The vegetation changes warmed the surface temperature by 0.037 °C decade^{-1} during 1982–2015.

GRAPHICAL ABSTRACT
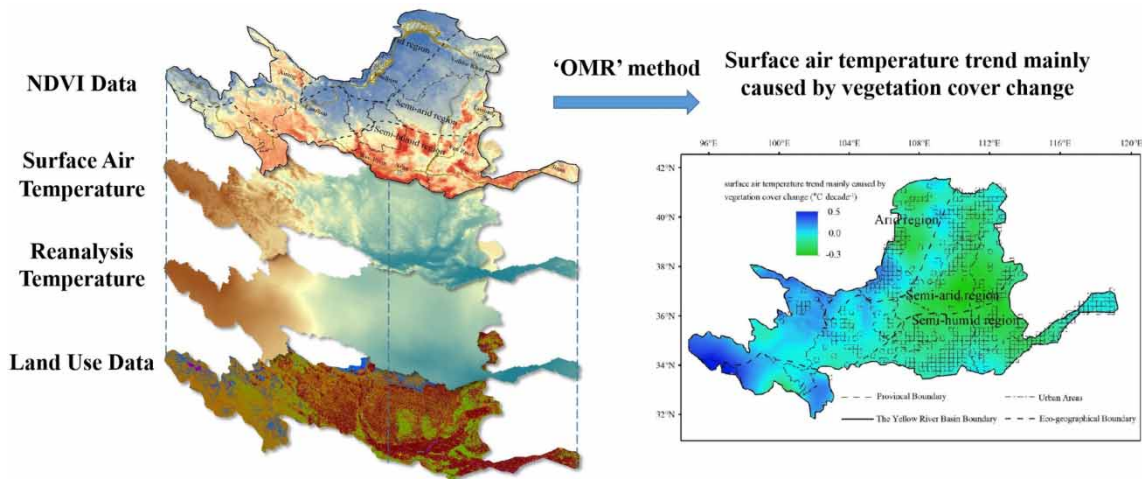
1. INTRODUCTION

The global surface temperature in the first two decades of the 21st century (2001–2020) was 0.99 °C higher than in 1850–1900, on average (IPCC 2021). The impact of human activities since industrialization on the global climate system has been further affirmed in the The Intergovernmental Panel on Climate Change (IPCC) AR6. As one of these human activities, land use/land cover change (LULC) influences the biophysical properties of the surface; the surface controls the exchange of moisture, kinetic energy, and energy in the atmosphere, which is finally expressed as local or even regional surface temperature change (Bonan 2008). Therefore, when a large-scale change in vegetation cover occurs in a certain area, it directly impacts the surface energy balance, which may cause warming or cooling effects on the area. Over the past 50 years, the Chinese government has promoted the implementation of a series of environmental protection projects, such as the Grain for Green Project, the construction of the Three-North Shelterbelt Program, and the protection of natural forest resources, which have led to a significant change in vegetation cover in the YRB (Hu *et al.* 2020; Lu *et al.* 2021). The spatio-temporal distribution of vegetation and its response to the climate in the Yellow River Basin (YRB) is an essential part of promoting the water and carbon cycle in the ecosystem and has consistently been a topic in recent scientific research (Guo *et al.* 2021; Ye *et al.* 2021). Such research provides reference and guidance for the implementation of China's afforestation strategy. However, few studies have reported the impact of vegetation cover changes on climate systems.

Surface air temperature (SAT) is a parameter that can characterize the physical process of a surface, and it is the driving factor in surface–atmosphere energy exchange. It was used to quantitatively evaluate the influence of vegetation on climate in this study. The effects of variation in vegetation on the change of SAT varied substantially among regions, with complex factors, playing warming or cooling roles. If regional vegetation coverage increases, vegetation reduces the albedo of the area. The absorption of more radiation is accompanied by a heating effect on the surface. An increase in vegetation coverage means a larger leaf area index and more severe transpiration, which is the main cause of the cooling effect of the surface (Chi *et al.* 2021). The dynamic balance of the two effects leads to overall heating or cooling effects of vegetation on SAT. Related studies have concluded that the effect of vegetation on SAT is influenced by complex factors, such as vegetation cover types, seasonal variations, and geographical location; consequently, different conclusions may be drawn from different studies. As early as 2010, Yang *et al.* (2010) classified the study area with the normalized difference vegetation index (NDVI) as the index and found that the heating effect on the surface was obvious with a low NDVI, but with the increase in the NDVI, the change in SAT gradually decreased and even exhibited a negative value. Liu *et al.* (2013) pointed out that vegetation variation is negatively correlated with SAT in eastern China, and the impact of vegetation on SAT differs at different latitudes (Wickham *et al.* 2012; Wang *et al.* 2014; Shen *et al.* 2015). To evaluate the effects of variation of vegetation on change in SAT in the middle latitudes, this study considered the YRB as the study area, and the dataset selected was Global Inventory Modeling and Mapping Studies (GIMMS) NDVI 3rd generation (NDVI3 g) V1.0 (Soomro *et al.* 2021). The aim was to provide scientific

evidence and support for the effect of vegetation variation on SAT in the middle latitudes, which may contribute to the development of vegetation construction policies.

One of the most commonly used methods for studying the influence of vegetation on climate is to build a climate model (Deborah Lawrence 2014). However, because of the coarse spatial resolution of a global climate model and the uncertainty of the physical processes, parameterization, and input data, a global climate model cannot reliably reproduce local climate effects. When data continuity and reliability are assured, the observation minus reanalysis (OMR) method can separate vegetation from complex factors and analyze local surface temperature changes. The OMR method can eliminate the changes in SAT caused by large-scale climate changes to allow the investigation of variation in vegetation (Kalnay & Cai 2003). The reanalysis data used in the OMR method can represent large-scale climate changes but are insensitive to regional surface processes because little or no surface data or information (surface observations of temperature, moisture, and wind overland) about land surface changes have been utilized in the data assimilation process (Wang & Yan 2015; Ao et al. 2020). Assuming that the LULC could affect the observed temperature, the difference between the reanalysis temperature and the observed temperature could indicate the influence of LULC on SAT change. After the basic idea of OMR was proposed in 2003, it was initially used to describe the impact of urbanization and land-use types on the SAT (Zhou et al. 2004; Lim et al. 2005). The application experiences have sped up the widespread application of OMR methods in research on the impact of LULC on climate in multiple countries and regions (Sun et al. 2011; Jin et al. 2020), which has verified the reliability of the OMR method. The current study uses the OMR method as the primary research method based on the observed SAT from the China Meteorological Data Service Center and ERA-interim reanalysis temperature.

The study aimed to analyze the temporal and spatial variation of vegetation in the YRB and the impact of vegetation change on SAT using the OMR method to provide theoretical support for understanding vegetation cover dynamics in the YRB and the bidirectional coupling between the atmosphere and vegetation.

2. MATERIALS AND METHODS

2.1. Study area

The YRB is in 95 °53′–119 °12′ E and 32 °9′–41 °50′ N with a basin area of 795,000 km² (Figure 1) (Miao et al. 2012). The terrain of the YRB is high in the west, low in the east, and the average elevation of the western area is above 4,000 m which is composed of a series of high mountains. The elevation of the central region is between 1,000 and 2,000 m, which is a loess landform with a serious threat of soil erosion, and the eastern part is only 100 m above sea level, which is mainly formed by the alluvial plain of the Yellow River (Jiang et al. 2015). The average annual precipitation ranges from 200 mm in the northwest to 750 mm in the south of the YRB (Li et al. 2019). According to the climatic region, the YRB is divided into arid, semi-arid, and semi-humid regions from north to south (Figure 1).

2.2. Methods

Considering that the impact of urbanization on SAT in the process of the global warming cannot be ignored, we extracted unurbanized areas for this study (IPCC 2007). For different buffer radii of meteorological observation stations, the correlation between annual temperature trends and urban land expansion varied with high correlation values at 10–20 km (Ge et al. 2013). This rule applied to grid data after the temperature was interpolated. The YRB was divided into 20 km²×20 km² using 1980 and 2015 land-use data; squares with changes in the construction land area fraction larger than 1% were defined as urban areas. The remaining areas were non-urban, allowing the sole consideration of the impacts of vegetation changes and background climate change on SAT.

This study used variations in NDVI, SAT, OMR, and ERA-interim reanalysis data as evaluation indexes when analyzing trends in the YRB and its three climate regions during 1982–2015 (He et al. 2017). This study analyzed the grid data of the YRB using the ordinary least-squares regression method to obtain the spatial distributions of Slope$_{NDVI}$, Slope$_{RT}$, and Slope$_{SAT}$. In addition, Slope$_{OMR}$ was obtained by 'Slope$_{SAT}$ minus Slope$_{RT}$'. The contribution of vegetation changes was quantified by the 'contribution rate of NDVI influence', which is the proportion of vegetation change with respect to temperature change (Ao et al. 2020).

To assess the impact of vegetation cover change on SAT change, the relationships between M_{NDVI} and Slpoe$_{OMR}$, Slope$_{NDVI}$, and Slope$_{OMR}$ were analyzed by using the correlation method. The methodology used in this study is illustrated in Figure 2.
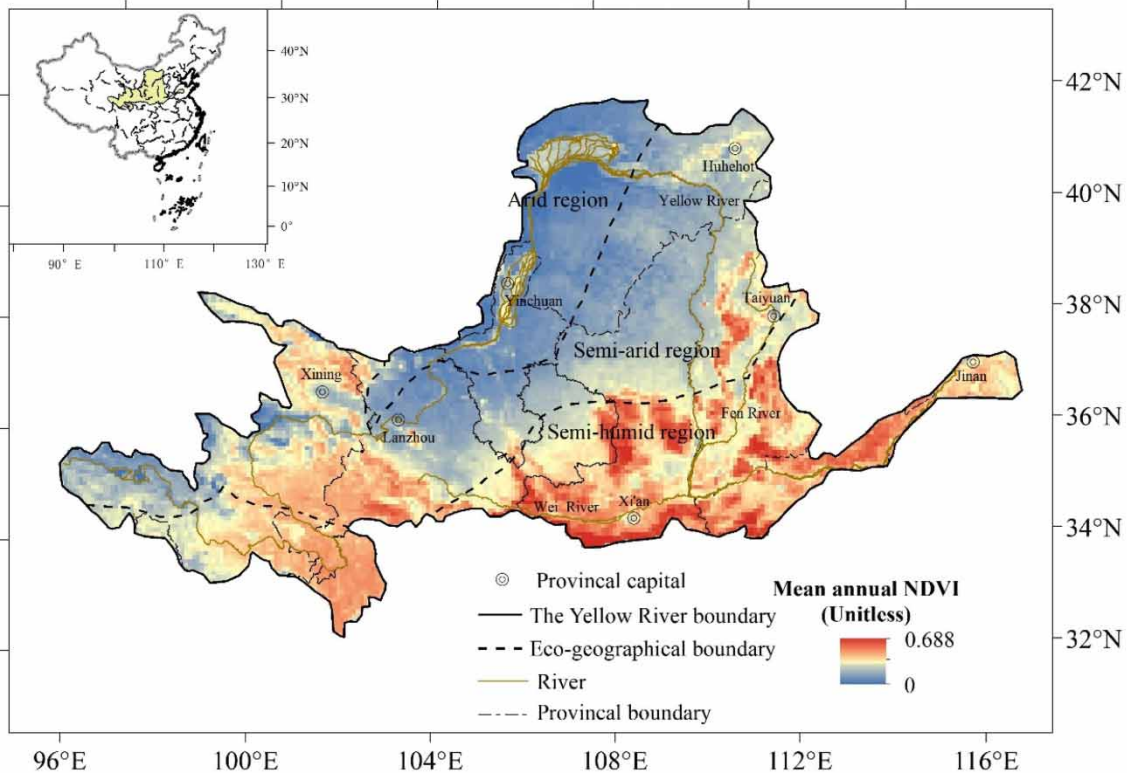
Figure 1 | The geographical location of the YRB and its three climatic sub-regions.
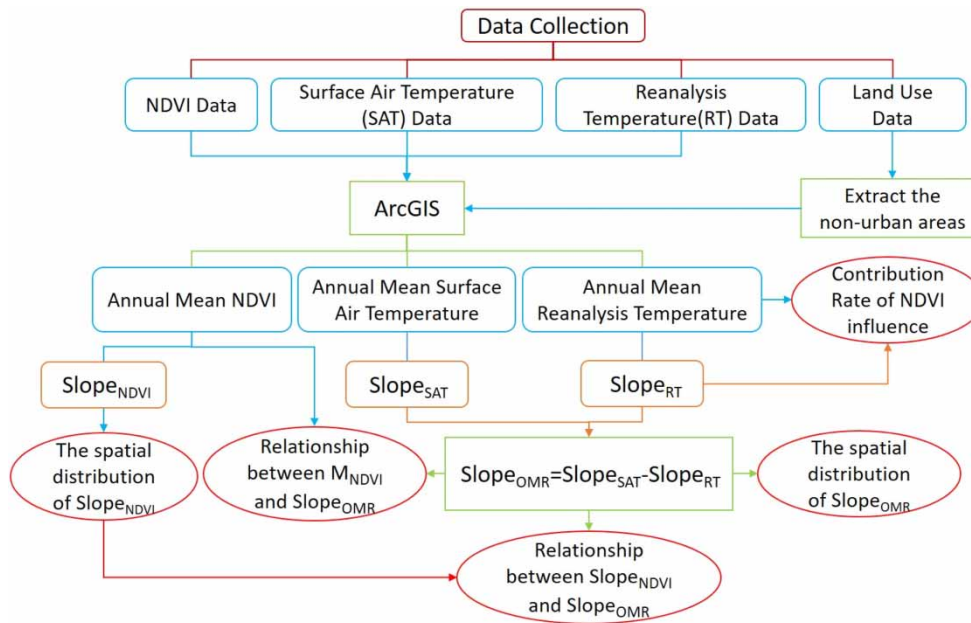

Figure 2 | The flowchart of data and analyses.

2.2.1. NDVI data

To quantify vegetation conditions, the NDVI data used in this study were the GIMMS NDVI3 g V1.0 dataset (Sun *et al.* 2021), which was obtained from the National Aeronautics and Space Administration (NASA) Ames Ecological Forecasting Lab (www.ecocast.arc.nasa.gov). The dataset was acquired by the advanced very high-resolution radiometer (AVHRR) of the National Oceanic and Atmospheric Administration (NOAA). It is one of the most extended NDVI time series globally, with a spatial resolution of 8 km and a temporal resolution of 15 days. In this study, data from 1982 to 2015 were selected for analysis (Ni *et al.* 2020; Zhai *et al.* 2020).

The dataset was processed in three steps: (1) the maximum value composite (MVC) method was used to merge the 15-day raster files into monthly NDVI data (Sun *et al.* 2021); (2) the mean annual NDVIs from 1982 to 2105 were obtained by averaging monthly NDVI values (Wu *et al.* 2020); (3) the actual value of the data ranged from −1 to 1. To eliminate the impact of other factors, the study focused on variation in vegetation. Grid cells with negative values were assigned the value of zero to eliminate the effects of water.

2.2.2. Surface air temperature data

The spatial interpolation dataset of the annual mean SAT in China was taken from the China Meteorological Data Service Center (http://data.cma.cn/en). The spatial interpolation dataset is based on the daily observation data of over 2,400 meteorological stations in China. It interpolated the data to a grid with a 1 km spatial resolution using the ANUSPLIN software (Zhou 2019). The annual mean SAT data from 1982 to 2015 in the YRB was applied for the study.

2.2.3. Reanalysis temperature data

Reanalysis data are insensitive to urbanization and land-use changes and are essential data for use in the OMR method (Wang *et al.* 2018). Given the spatial resolution and time-series length, we selected the ERA-interim dataset from the European Centre for Medium-range Weather Forecasts (https://www.ecmwf.int/). To ensure the reliability of the ERA-interim reanalysis temperature data in the YRB (Zhao *et al.* 2020), we calculated the correlation coefficient between SAT and the reanalysis air temperature in the YRB. The spatial distribution of the correlation coefficients between the two types of temperature data is shown in Figure 3.

The annual mean reanalysis of air temperature with a spatial resolution of 7.5 arc min was calculated from the monthly means of daily means 2 m temperature data. Because of the different spatial resolutions of the datasets, the bilinear interpolation method was used to resample and unify the data resolution for better subsequent data analysis.
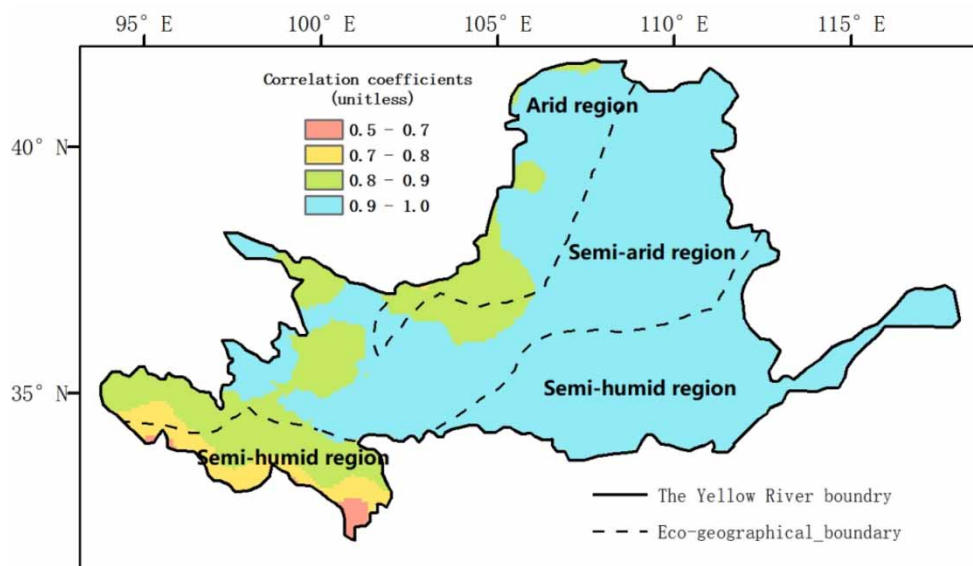

Figure 3 | The spatial distribution of correlation coefficients between observed temperatures and ERA-interim reanalysis during 1982–2015 in the YRB.

2.2.4. Land-use data

To extract the areas affected by urbanization in the YRB from 1982 to 2015, we selected land-use data with resolving 1 km provided by the Data Center for Resources and Environmental Sciences (https://www.resdc.cn). Land-use data for 1980 and 2015 were generated by manual visual interpretation using the Landsat thematic mapper (Landsat TM)/enhanced thematic mapper (ETM) and Landsat8 remote sensing images (Deng *et al.* 2015). These data serve as the basis for determining the urbanization areas and non-urbanization areas.

3. RESULTS

3.1. Excluding the SAT impact of urbanization

Land use in the YRB was roughly divided into six types such as grassland, farmland, forest, constructed land, water, and unused land, among which grassland and farmland areas accounted for the largest percentages of the YRB, at for almost half and one-quarter of the total area, respectively (Figure 4). A comparison of land-use data in the 1980s and 2015 showed that the areas of grassland, constructed land, water, and farmland decreased to different degrees, and the forest area and urbanization areas increased to varying degrees (Table 1). The percentage of urbanized areas increased by 0.9%. The final calculations show that the urban and non-urban areas in the YRB accounted for 24 and 76% of the total basin area, respectively. Urbanized areas are concentrated in the central and eastern regions of the YRB. Figure 5 shows that urbanization is more significant near the provincial capital urban agglomeration, and the percentage of urban areas in some grids is over 5%.

3.2. Vegetation dynamics

Figure 6(a) shows the annual mean NDVI variation trend in the YRB from 1982 to 2015. The NDVI variation trend spread from -3.5 to 4.8 (10^{-2} decade^{-1}). Vegetation in the southeast triangular area shows an obvious growth trend, while vegetation recovery in the western and northwestern areas is poor and has a decreasing trend in some areas. Areas with obvious degeneration in vegetation cover were mainly concentrated in urban areas.
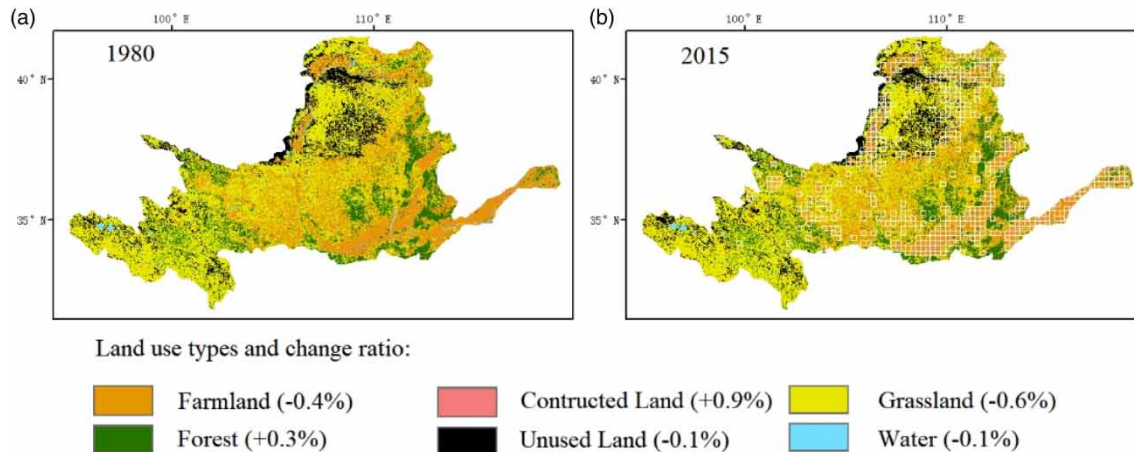

Figure 4 | The spatial distribution of land-use types in: (a) 1980 and (b) 2015 in the YRB. The regions in the white squares are areas that experienced urbanization between 1980 and 2015.

Table 1 | Percentage of land-use types in 1980 and 2015

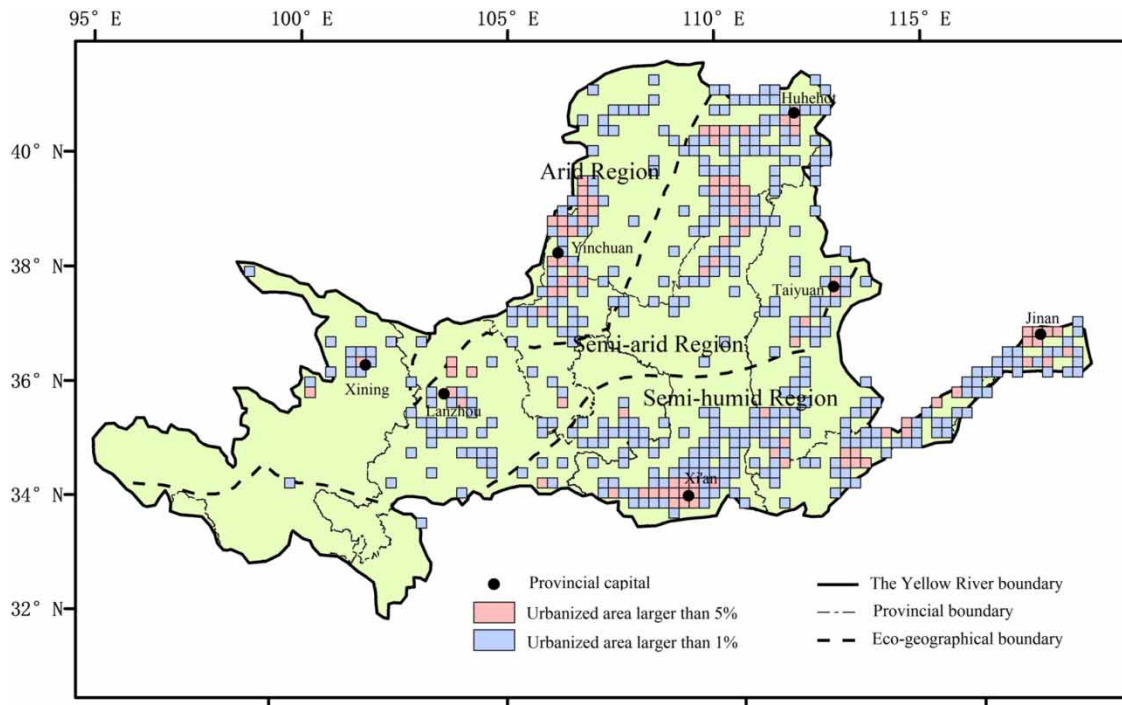|	Farmland	Forest	Grassland	Water	Constructed land	Unused land
1980 (%)	26.2	12.8	48.1	1.8	2	9.1
2015 (%)	25.8	13.1	47.5	1.7	2.9	9

Figure 5 | The spatial distribution of urban and non-urban areas in the YRB.

Figure 6(b) shows the trend of OMR temperature change in the YRB, with $\text{Slope}_{\text{OMR}}$ values between -0.3 and $0.5\,°C$ decade^{-1}. The OMR temperature in the southeastern triangular area declined, and the north of the arid region also showed a clear downward trend. The OMR temperature west of the YRB exhibited an upward trend.

3.3. Temporal changes in the NDVI and temperature

Figure 7(a)–7(d) describes the inter-annual changes of the mean annual NDVI (M_{NDVI}) from 1982 to 2015 in the YRB and the three climatic regions. Figure 7(a) shows that the YRB NDVI fluctuated between 0.29 and 0.35, with an average growth trend of 0.11 decade^{-1}. The annual mean NDVI trend ($\text{Slope}_{\text{NDVI}}$) of the three climatic sub-regions was estimated to be 0.59×10^{-2}, 1.11×10^{-2}, and 1.32×10^{-2} decade^{-1} in the arid, semi-arid, and semi-humid regions, respectively.

Similarly, Figure 7(e)–7(h) describes the changing trends of observed and reanalyzed temperatures. The changing trends in the two types of datasets were consistent, and the annual mean reanalysis temperature was higher than the annual mean surface observation temperature. The temperature of the YRB had clear upward trends of between 0.40 and 0.50 °C decade^{-1} in different climate regions.

Figure 7(i)–7(l) shows the change in the OMR temperature, which is caused by changes in vegetation. The trend of increasing OMR temperature in the YRB was 0.04 °C decade^{-1} ($R^2 = 0.11716$; Figure 7(i)). The OMR trends ($\text{Slope}_{\text{OMR}}$) in the three climatic sub-regions were estimated to be 0.023, 0.024, and 0.047 °C decade^{-1} in the arid, semi-humid, and semi-arid regions, respectively. The R^2 for the arid, semi-arid, and semi-humid regions were 0.02427, 0.15167, and 0.04142, respectively.

The impact of variations in the NDVI on SAT was consistent across the YRB (Table 2). The YRB $\text{Slope}_{\text{OMR}}$ was 0.037 °C decade^{-1}, contributing 7.62% to the SAT. Among the three climate regions, the contribution of NDVI influence was highest in semi-arid areas, accounting for 9.36%, followed by arid and semi-humid areas, with contributions of 5.35 and 5.05%, respectively. This means that the contribution of vegetation change to SAT in the YRB was no greater than 10%.

3.4. Relationship between the NDVI and OMR temperature

Figure 8(a) shows the negative correlation between the M_{NDVI} and the $\text{Slope}_{\text{OMR}}$ in the YRB ($r = -0.095$, $P < 0.001$), with an average M_{NDVI} value of 0.32. This rule applies equally to the semi-arid and semi-humid regions. Figure 8(c) and 8(d) shows
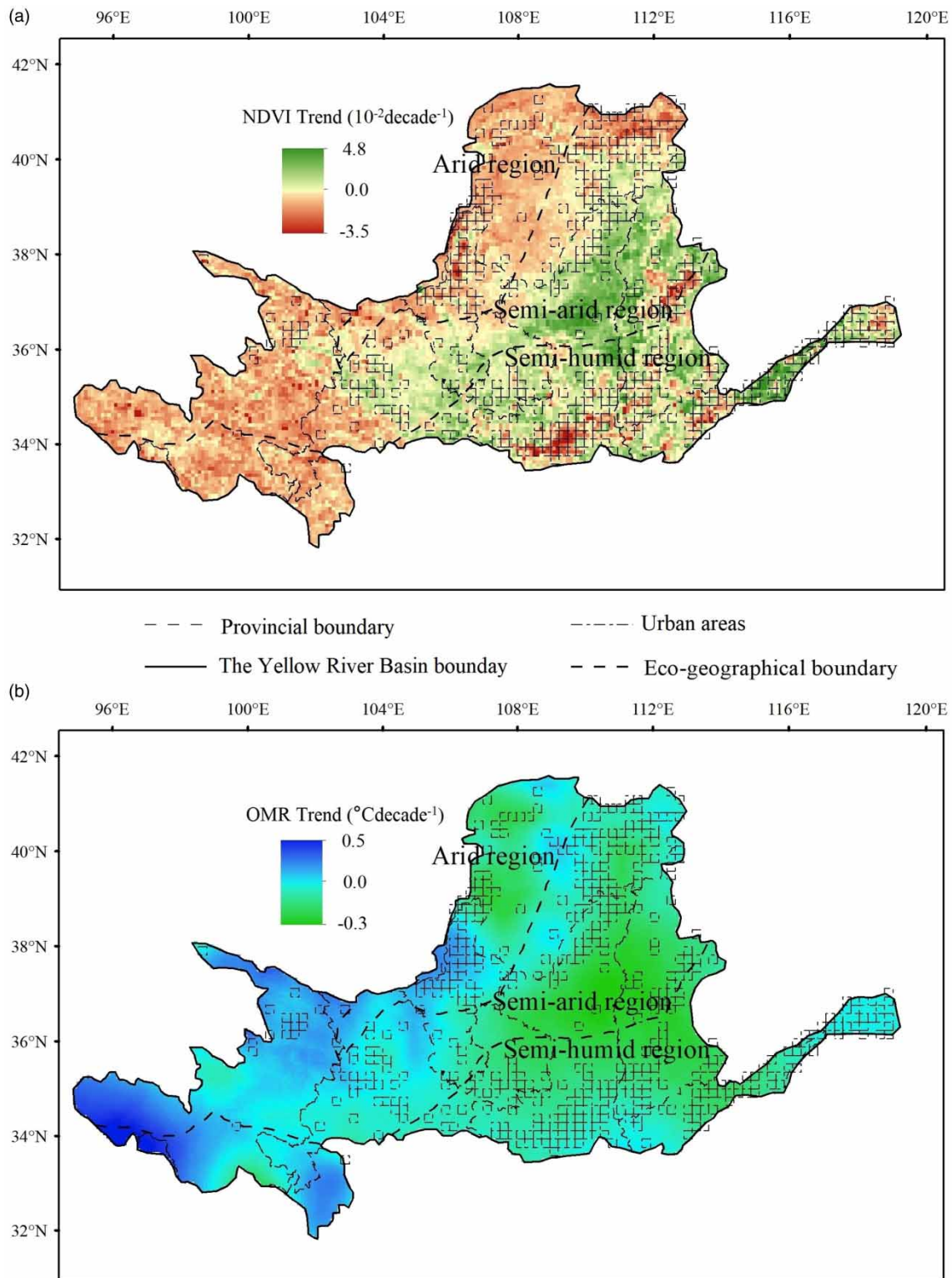
Figure 6 | The spatial distribution of: (a) NDVI trend (Slope$_{NDVI}$) and (b) OMR temperature trend (Slope$_{OMR}$) in the YRB during 1982–2015.

that this negative correlation was more significant in the sub-humid region (average $M_{NDVI} = 0.45$), with a correlation coefficient of $r = -0.267$ ($P < 0.001$). The equivalent correlation coefficient in the semi-arid region was -0.067 ($P < 0.05$), with the vegetation cover of the average M_{NDVI} being 0.29.
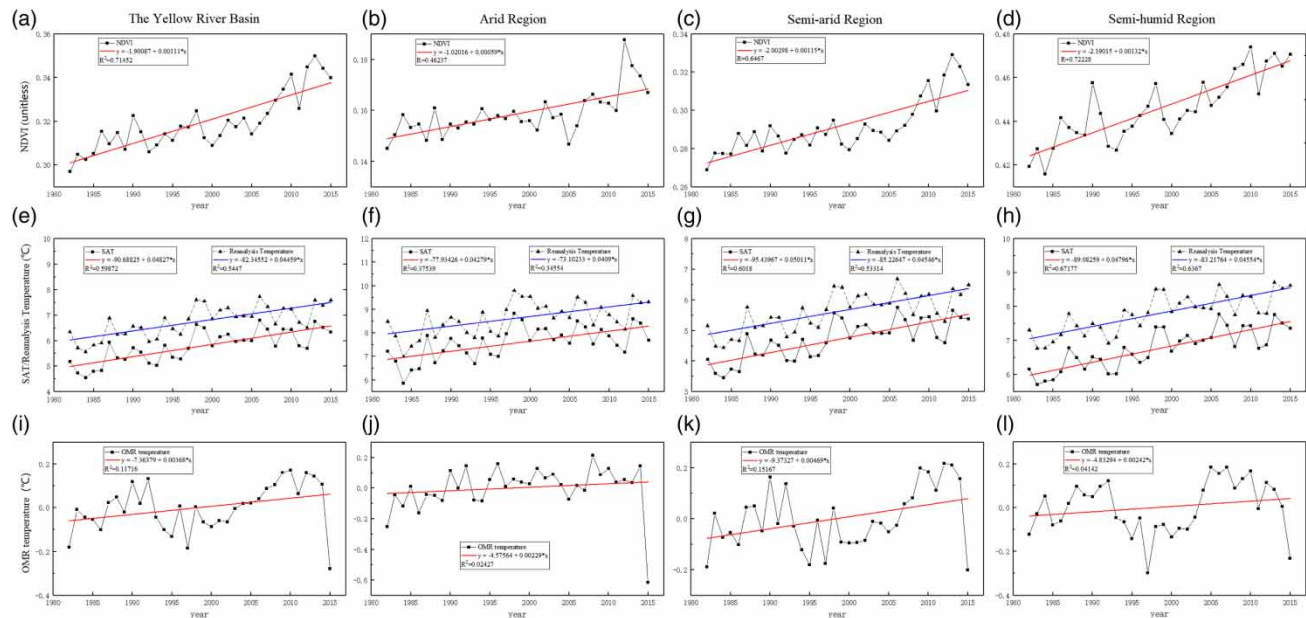
Figure 7 | The inter-annual variation of the annual mean NDVI from 1982 to 2015 on: (a) the Yellow River Basin (YRB) and its (b) arid; (c) semi-arid; and (d) semi-humid regions. The inter-annual variation of annual mean SAT and reanalysis temperatures during 1982–2015 in (e) the YRB and its (f) arid, (g) semi-arid; and (h) semi-humid regions. The blue and red lines refer to the linear trends of SAT and reanalysis temperature, respectively. (i)–(l) refer to the inter-annual variation in annual mean OMR temperature from 1982 to 2015 in the YRB, arid, semi-arid–, and semi-humid regions. Please refer to the online version of this paper to see this figure in colour: http://dx.doi.org/10.2166/wcc.2022.037.

Table 2 | NDVI trend ($Slope_{NDVI}$), OMR trend ($Slope_{OMR}$), SAT trend ($Slope_{SAT}$), and contribution rate of NDVI influence of non-urban region during 1982–2015

1982–2015	The Yellow River Basin	Arid region	Semi-arid region	Semi-humid region
$Slope_{NDVI}$ (10^{-2} decade^{-1})	1.11	0.59	1.15	1.32
$Slope_{OMR}$ (°C decade^{-1})	0.037	0.023	0.047	0.024
$Slope_{SAT}$ (°C decade^{-1})	0.48	0.43	0.50	0.48
Contribution rate of NDVI influence (%)	7.62	5.35	9.36	5.05

Note: Contribution rate of NDVI influence = $Slope_{OMR}$/$Slope_{SAT}$*100%.

In the non-urban areas of the YRB from 1982 to 2015, $Slope_{OMR}$ decreased (Figure 8(e)), with a $Slope_{NDVI}$ negative correlation coefficient of -0.582 ($P < 0.001$). In addition, the percentage of grids with $Slope_{OMR}$ less than and larger than 0 decade^{-1} was approximately 38 and 62%, respectively. Figure 8(g) and 8(h) shows that a negative correlation still occurred between $Slope_{NDVI}$ and $Slope_{OMR}$ in the semi-arid and semi-humid regions, with correlation coefficients of -0.702 ($P < 0.001$) and -0.589 ($P < 0.001$), respectively. However, $Slope_{NDVI}$ and $Slope_{OMR}$ in arid regions were positively correlated, with a correlation coefficient of 0.142 ($P < 0.01$). The ratio of a grid with $Slope_{OMR}$ was less or larger than 0 decade^{-1}. The greatest imbalances in the semi-arid regions were 68 and 32%, respectively. Semi-humid regions were more uniform with 54 and 46% ratios, and the ratio in arid regions was in the middle with 60 and 40%, respectively.

4. DISCUSSION

4.1. Vegetation cover and SAT change over the YRB

Based on NDVI data from 1982 to 2015, this study analyzed the spatial and temporal variation of vegetation in non-urban areas of the YRB. The results show that the vegetation change trend in the YRB was 1.11×10^{-2} decade^{-1} from 1982 to 2015, which is similar to the vegetation change trend of 1.58×10^{-2} decade^{-1} in the same period in the Loess Plateau (Jin
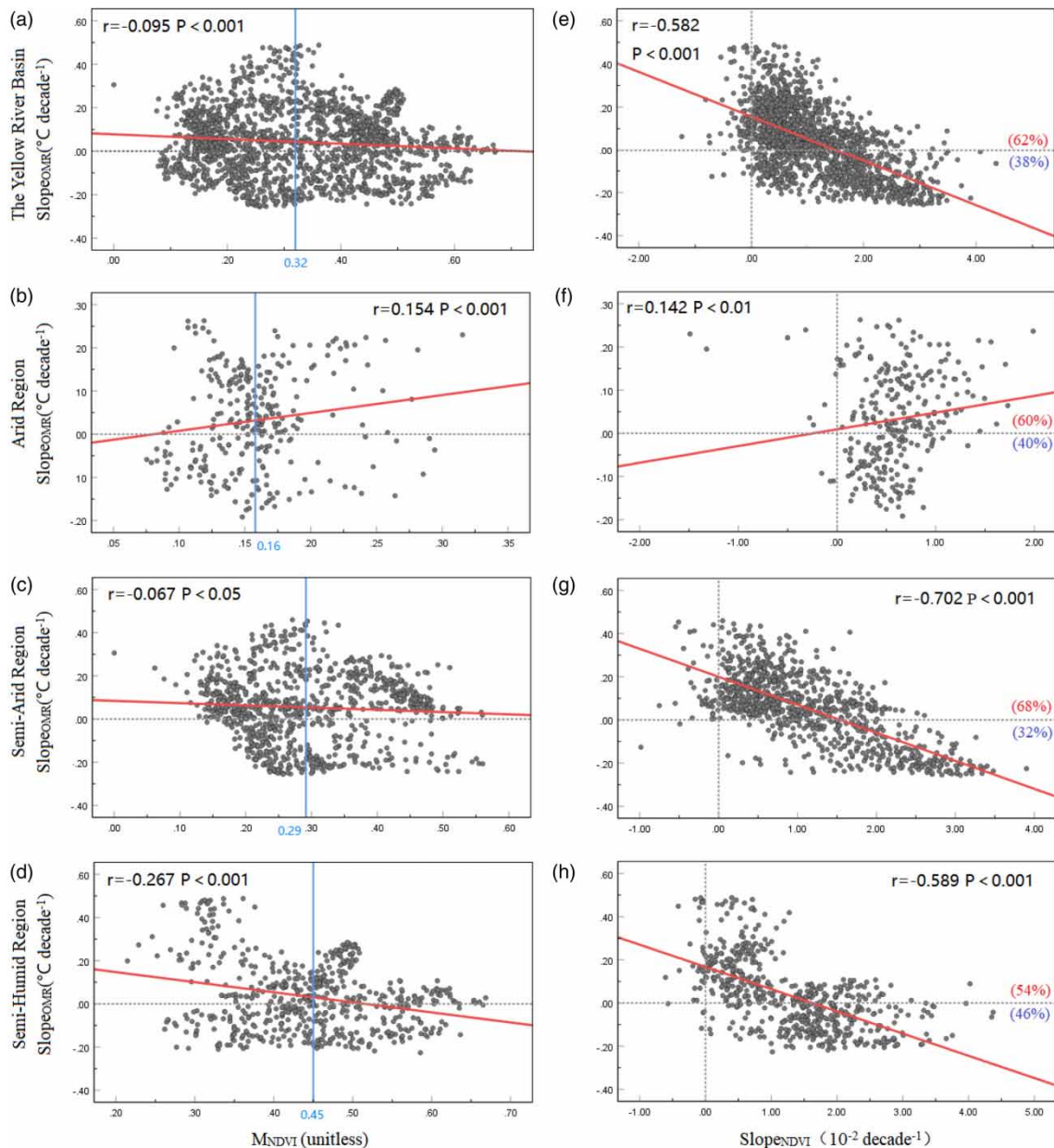
Figure 8 | (a)–(d) Scatter diagrams between the Slope$_{OMR}$ and mean annual NDVI (M_{NDVI}) during 1982–2015 in (a) the YRB; (b) arid region; (c) semi-arid region; and (d) semi-humid region. The blue lines represent the mean annual NDVI. (e) and (f) Scatter diagrams between the Slope$_{OMR}$ and the Slope$_{NDVI}$ during 1982–2015 in (e) the YRB; (f) arid region; (g) semi-arid region; and (h) semi-humid region. The figures in blue and red colors represent the percent of the grids, with Slope$_{OMR}$ being larger and less than 0 decade^{-1}, respectively. Please refer to the online version of this paper to see this figure in colour: http://dx.doi.org/10.2166/wcc.2022.037.

et al. 2020). The difference between the results was caused by large spatial differences in vegetation cover in the YRB. The source of the Yellow River is on the Qinghai-Tibet Plateau, where the vegetation trend is much lower than that in the central and eastern regions of the YRB (Guan et al. 2015; Ma et al. 2018). Compared with the global NDVI change trend, which was 0.46×10^{-2} decade^{-1} in 1982–2012, the vegetation change trend in the YRB was much higher. It demonstrates the effectiveness of a series of ecological environmental protection policies implemented by the Chinese government (Liu et al. 2015). Recapping vegetation in the arid region of the YRB was poor and showed the lowest changing trend (Slope$_{NDVI}$ = 0.59×10^{-2} decade^{-1}). However, the trend was still higher than the result for NDVI during the 1982–2013 growth season in

Inner Mongolia, which was $\text{Slope}_{\text{NDVI}} = 0.3 \times 10^{-2}$ decade^{-1} (Tong *et al.* 2017). The differences between these studies and Tong's results are related to the climate sub-region division pattern, whether urbanized areas are excluded and how the annual mean NDVI is calculated.

The trend of temperature change in the YRB affected by vegetation changes during 1982–2015 was 0.037 °C decade^{-1}, which showed that vegetation restoration in the YRB had a heating effect on SAT. The heating impact of vegetation change on the surface is mainly due to the radiation effect. An increase in vegetation leads to a decrease in albedo, which manifests as a heating effect. Vegetation restoration in the YRB is mainly manifested in the expansion of the forest, and the albedo of the forest is lower than those of grassland and farmland, which may be a cause of local warming.

In the YRB, although the NDVI changes varied in different climate regions from 1982 to 2015, the contributions of NDVI influences were similar and concentrated between 5 and 10%. This means that among the factors affecting the SAT, the effects of vegetation cover changes were limited, and their impact was not dominant among the many complicated factors. The change in SAT may be mainly derived from the change in the climate background and the increase in carbon dioxide emissions caused by human activities (IPCC 2021).

4.2. Analysis of the relationship between vegetation change and SAT change

The difference between the observed and reanalyzed temperatures was used to determine the temperature affected by vegetation change using the OMR method. According to the results, the NDVI (M_{NDVI}) in the YRB was negatively correlated with the $\text{Slope}_{\text{OMR}}$ (Ning *et al.* 2017). However, the correlation between M_{NDVI} and $\text{Slope}_{\text{OMR}}$ was not always negative in different climate regions. The negative correlation ($r = -0.067$) was already very weak when the mean M_{NDVI} was 0.29 in a semi-arid region. When the average value of M_{NDVI} reached only 0.16 in the arid region, M_{NDVI} and $\text{Slope}_{\text{OMR}}$ showed a weak positive correlation ($r = 0.154$). This study showed that when the vegetation coverage reached a certain degree, the better the vegetation coverage was, and the more restrained the warming effect on SAT. When the vegetation coverage level was low, the influence of vegetation on SAT was less consistent and showed a certain regionality.

In Liu's research, the OMR temperature showed a cooling trend in eastern China when the annual mean NDVI was greater than 0.55 (Liu *et al.* 2013). However, the value of M_{NDVI} in semi-humid areas with the best coverage in the YRB reached only 0.45. Therefore, the cooling effect of vegetation restoration on the SAT has not yet been confirmed. Although the results still showed a warming effect ($\text{Slope}_{\text{OMR}} = 0.024$ °C decade^{-1}) on the surface, the negative correlation between $\text{Slope}_{\text{NDVI}}$ and $\text{Slope}_{\text{OMR}}$ was consistent with the findings of Liu.

With respect to exploring the correlation between $\text{Slope}_{\text{NDVI}}$ and $\text{Slope}_{\text{OMR}}$, we found a significant negative correlation in semi-arid and semi-humid regions with high latent heat exchange levels and a positive correlation in arid regions with significant sensible heat exchange. In addition, rapid vegetation restoration in areas with suitable vegetation cover may have a cooling effect on SAT.

The heating and cooling effects of vegetation change on SAT are dynamic. Areas with sparse vegetation have higher levels of sensible heat exchange. When the heat cannot be absorbed by sufficient water evaporation, it accumulates on the earth's surface, and the SAT is higher. With the improvement in vegetation cover, sensible heat exchange is gradually replaced by latent heat exchange, and the transpiration of vegetation increases to achieve the effect of cooling the SAT (Gou *et al.* 2018). However, the improvement in vegetation cover will lead to a decrease in surface reflectivity because the albedo of bare land is higher than that of vegetation. Areas with increased vegetation cover absorbed more solar radiation, which had a warming effect on the surface. The two effects interact in the dynamic response of SAT to vegetation changes. The YRB is a geographically diverse river basin with specific spatial differences in vegetation types, and cover levels are one reason for the observed differences in relationships among the different study regions.

The analyses in this study were based on different climatic conditions. However, the YRB has a wide range of complex terrains. The relationship between vegetation and temperature cannot be completely described based on the division of climate characteristics. In subsequent studies, taking vegetation type or land-use type as the basis for division will be a direction for future work.

5. CONCLUSION

Based on the OMR method, we analyzed the spatio-temporal variation of vegetation cover and its impact on SAT change in non-urban areas of the YRB from 1982 to 2015. This provides a basis for understanding the characteristics of vegetation cover

in the YRB. It also provides a reference for deepening the understanding of the coupling relationship between vegetation and climate.

The vegetation cover in the YRB showed clear spatial differences. Areas with suitable vegetation cover were mainly concentrated in the southeastern triangle of the basin. The source of the Yellow River and the northwestern region of the basin are poor. In the time series of this study, the change trends of the NDVI increased from north to south. The change trends in the arid, semi-arid, and semi-humid regions were estimated to be 0.59, 1.15, and 1.32×10^{-1} decade^{-1}, respectively. Overall, the recovery rate of the YRB was 1.11×10^{-1} decade^{-1}. Thus, the vegetation recovery results were more significant in wetter regions.

During the 34 years from 1982 to 2015, SAT in the YRB showed a warming trend of 0.48 °C decade^{-1}. The temperature change trend affected by vegetation was 0.037 °C decade^{-1}, with a contribution of 7.62% by the NDVI. Vegetation changes had different warming effects on the surface temperature over the three climatic regions, with the results of Slope$_{OMR}$ in arid, semi-arid, and semi-humid areas being 0.023, 0.047, and 0.024 °C decade^{-1}, respectively. These results show that vegetation changes in the YRB from 1982 to 2015 had warming effects on the SAT, but the contribution of NDVI was not high (less than 10%). Therefore, the restoration of vegetation guided by a series of vegetation restoration policies in the YRB has neither had a significant impact on the local climate nor is it the main reason for the warming of the YRB.

After exploring the correlation between NDVI and SAT, the following conclusions were drawn: the strong negative correlations among M_{NDVI}, Slope$_{NDVI}$, and Slope$_{OMR}$ can be used as a reference only in areas with good vegetation coverage. In areas with general vegetation coverage and even poor conditions, such as the arid region of the YRB divided in this study, this negative correlation is not obvious with only a weak correlation; this correlation law has strong regional characteristics. Therefore, local vegetation coverage and climate conditions should be fully considered when formulating policies such as regional vegetation protection.

AUTHORS CONTRIBUTIONS

For this research paper with several authors, a short paragraph specifying their individual contributions was provided. Z.H. developed the original idea and contributed to the research design for the study. Q.W. was responsible for data collection. C.H. and R.L. provided guidance and contributed to the research design. D.H. and S.-S. provided guidance for the writing of the article. All authors have read and approved the final manuscript.

DATA AVAILABILITY STATEMENT

Data cannot be made publicly available; readers should contact the corresponding author for details.

CONFLICT OF INTEREST

The authors declare there is no conflict.

REFERENCES

Ao, X., Zhai, Q.-f., Cui, Y., Zhou, X.-y., Zhao, C.-y., Zhang, J.-g. & Yuan, J. 2020 Analysis of the influence of urbanization process on the temperature change in Liaoning province based on the OMR method. *Journal of Meteorology and Environment* **36**, 28–35 (in Chinese).

Bonan, G. B. 2008 Forests and climate change: forcings, feedbacks, and the climate benefits of forests. *Science* **320**, 1444–1449.

Chi, Q., Zhou, S., Wang, L., Zhu, M., Liu, D., Tang, W., Cui, Y. & Lee, J. 2021 Exploring on the eco-climatic effects of land use changes in the influence area of the Yellow River basin from 2000 to 2015. *Land* **10**, 601.

Deborah Lawrence, K. V. 2014 Effects of tropical deforestation on climate and agriculture. *Nature Climate Change* **5**, 27–36.

Deng, X., Shi, Q., Zhang, Q., Shi, C. & Yin, F. 2015 Impacts of land use and land cover changes on surface energy and water balance in the Heihe River Basin of China, 2000–2010. *Physics and Chemistry of the Earth, Parts A/B/C* **79–82**, 2–10.

Ge, Q., Wang, F. & Luterbacher, J. 2013 Improved estimation of average warming trend of China from 1951–2010 based on satellite observed land-use data. *Climatic Change* **121**, 365–379.

Gou, J., Wang, F., Jin, K. & Dong, Q. 2018 Cooling effect induced by vegetation restoration on the Loess Plateau. *Acta Ecologica Sinica* **38**, 3970–3978 (in Chinese).

Guan, Y., Guo, S., Zhu, X., Zhang, L., Sielmann, F., Fraedrich, K. & Cai, D. 2015 Vegetation dynamics on the Tibetan plateau (1982–2006): an attribution by ecohydrological diagnostics. *Journal of Climate* **28**, 4576–4584.

Guo, Y., Zeng, J., Wu, W., Hu, S., Liu, G., Wu, L. & Bryant, C. R. 2021 Spatial and temporal changes in vegetation in the Ruoergai Region, China. *Forests* **12**, 76.

He, B., Chen, A., Jiang, W. & Chen, Z. 2017 The response of vegetation growth to shifts in trend of temperature in China. *Journal of Geographical Sciences* **27**, 801–816.

Hu, C., Zhang, L., Wu, Q., Soomro, S.-e-h. & Jian, S. 2020 Response of LULC on runoff generation process in middle Yellow River basin: the Gushanchuan basin. *Water* **12**, 1237.

IPCC 2007 *Summary for Policymakers, Climate Change 2007: The Physical Science Basis, Formally Approved at the 10th Session of Working Group I of the IPCC*. Cambridge University Press, Cambridge.

IPCC 2021 *Summary for Policymakers, Climate Change 2021: The Physical Science Basis, Contribution of Working Group I to the Fifth Assessment Report of the Intergovernmental Panel on Climate Change*. Cambridge University Press, Cambridge and New York.

Jiang, W., Yuan, L., Wang, W., Cao, R., Zhang, Y. & Shen, W. 2015 Spatio-temporal analysis of vegetation variation in the Yellow River Basin. *Ecological Indicators* **51**, 117–126.

Jin, K., Wang, F., Zong, Q., Qin, P. & Liu, C. 2020 Impact of variations in vegetation on surface air temperature change over the Chinese Loess Plateau. *Science Total Environment* **716**, 136967.

Kalnay, E. & Cai, M. 2003 Impact of urbanization and land-use change on climate. *Nature* **423**, 528–531.

Li, Y., Xie, Z., Qin, Y. & Zheng, Z. 2019 Responses of the Yellow River Basin vegetation: climate change. *International Journal of Climate Change Strategies and Management* **11**, 483–498.

Lim, Y.-K., Cai, M., Kalnay, E. & Zhou, L. 2005 Observational evidence of sensitivity of surface climate changes to land types and urbanization. *Geophysical Research Letters* **32**, n/a–n/a.

Liu, X., Wang, H., Shi, X. & Song, S. 2013 Impact of vegetation cover on surface temperature variation in East China. *Journal of PLA University of Science and Technology (Natural Science Edition)* **14**, 585–590 (in Chinese).

Liu, Y., Li, Y., Li, S. & Motesharrei, S. 2015 Spatial and temporal patterns of global NDVI trends: correlations with climate and human factors. *Remote Sensing* **7**, 13233–13250.

Lu, C., Hou, M., Liu, Z., Li, H. & Lu, C. 2021 Variation characteristic of NDVI and its response to climate change in the middle and upper reaches of Yellow River Basin, China. *IEEE Journal of Selected Topics in Applied Earth Observations and Remote Sensing* **14**, 8484–8496.

Ma, S., Bao, G. & Guo, G. 2018 Change trend of vegetation and its responses to climate change in the source region of the Yellow River. *Journal of Arid Meteorology* **36**, 226–233 (in Chinese).

Miao, C. Y., Yang, L., Chen, X. H. & Gao, Y. 2012 The vegetation cover dynamics (1982–2006) in different erosion regions of the Yellow River Basin, China. *Land Degradation & Development* **23**, 62–71.

Ni, Y., Zhou, Y. & Fan, J. 2020 Characterizing spatiotemporal pattern of vegetation greenness breakpoints on Tibetan plateau using GIMMS NDVI3 g dataset. *IEEE Access* **8**, 56518–56527.

Ning, J., Gao, Z., Meng, R., Xu, F. & Gao, M. 2017 Analysis of relationships between land surface temperature and land use changes in the Yellow River Delta. *Frontiers of Earth Science* **12**, 444–456.

Shen, X., Liu, B., Li, G., Yu, P. & Zhou, D. 2015 Impacts of grassland types and vegetation cover changes on surface air temperature in the regions of temperate grassland of China. *Theoretical and Applied Climatology* **126**, 141–150.

Soomro, S.-e-h., Hu, C., Jian, S., Wu, Q., Boota, M. W. & Aamir Soomro, M. H. A. 2021 Precipitation changes and their relationships with vegetation responses during 1982–2015 in Kunhar River basin, Pakistan. *Water Supply* **21** (7), 3657–3671.

Sun, M., Tang, J.-P. & Xu, C.-Y. 2011 Impact of urbanization and land-use change on regional temperature in eastern China. *Journal of Nanjing University (Natural Sciences)* **47**, 679–691 (in Chinese).

Sun, R., Chen, S. & Su, H. 2021 Climate dynamics of the spatiotemporal changes of vegetation NDVI in Northern China from 1982 to 2015. *Remote Sensing* **13**, 187.

Tong, S., Zhang, J., Bao, Y., Wurina, Terigele, Weilisi & Lianxiao, 2017 Spatial and temporal variations of vegetation cover and the relationships with climate factors in Inner Mongolia based on GIMMS NDVI3 g data. *Journal of Arid Land* **9**, 394–407.

Wang, M. & Yan, X. 2015 A comparison of two methods on the climatic effects of urbanization in the Beijing-Tianjin-Hebei metropolitan area. *Advances in Meteorology* **2015**, 1–12.

Wang, Q., Riemann, D., Vogt, S. & Glaser, R. 2014 Impacts of land cover changes on climate trends in Jiangxi province China. *International Journal of Biometeorology* **58**, 645–660.

Wang, J., Yan, Z. & Feng, J. 2018 Exaggerated effect of urbanization in the diurnal temperature range via 'Observation minus reanalysis' and the physical causes. *Journal of Geophysical Research: Atmospheres* **123**, 7223–7237.

Wickham, J. D., Wade, T. G. & Riitters, K. H. 2012 Comparison of cropland and forest surface temperatures across the conterminous United States. *Agricultural and Forest Meteorology* **166–167**, 137–143.

Wu, S., Gao, X., Lei, J., Zhou, N. & Wang, Y. 2020 Spatial and temporal changes in the normalized difference vegetation index and their driving factors in the desert/grassland biome transition zone of the Sahel Region of Africa. *Remote Sensing* **12**, 4119.

Yang, X., Zhang, Y., Ding, M., Liu, L., Wang, Z. & Gao, D. 2010 Observational evidence of the impact of vegetation cover on surface air temperature change in China. *Chinese Journal of Geophysics* **53**, 833–841.

Ye, W., van Dijk, A. I. J. M., Huete, A. & Yebra, M. 2021 Global trends in vegetation seasonality in the GIMMS NDVI3 g and their robustness. *International Journal of Applied Earth Observation and Geoinformation* **94**, 102238.

Zhai, X., Liang, X., Yan, C., Xing, X., Jia, H., Wei, X. & Feng, K. 2020 Vegetation dynamic changes and their response to ecological engineering in the Sanjiangyuan region of China. *Remote Sensing* **12**, 4035.

Zhao, P., Gao, L., Wei, J., Ma, M., Deng, H., Gao, J. & Chen, X. 2020 Evaluation of ERA-interim air temperature data over the Qilian Mountains of China. *Advances in Meteorology* **2020**, 1–11.

Zhou, Y. 2019 Asymmetric behavior of vegetation seasonal growth and the climatic cause: evidence from long-term NDVI dataset in Northeast China. *Remote Sensing* **11**, 2107.

Zhou, L. M., Dickinson, R. E., Tian, Y. H., Fang, J. Y., Li, Q. X., Kaufmann, R. K., Tucker, C. J. & Myneni, R. B. 2004 Evidence for a significant urbanization effect on climate in China. *Proceedings of the National Academy of Sciences of the United States of America* **101**, 9540–9544.